Tellus (1981), *33*, 372–381

An atmospheric radiative-convective model with interactive water vapor transport and cloud development

By JOHN R. HUMMEL[1] and WILLIAM R. KUHN, *Department of Atmospheric and Oceanic Science, The University of Michigan, Ann Arbor, Michigan 48109, U.S.A.*

(Manuscript received October 9, 1979; in final form September 4, 1980)

ABSTRACT

In the present generation of radiative-convective models, clouds are assigned specific levels or temperatures that do not change during the course of the calculations. In addition, a single water vapor distribution is used for the "mean atmosphere" instead of separate distributions for the clear sky and cloudy sky atmospheres. We present results from a one-dimensional radiative-convective model that includes interactive water vapor transport and predicts cloud altitudes and thicknesses.

The fully interactive model and one with a single, fixed cloud with a single water vapor profile can both reproduce a mean global temperature profile, their surface temperatures agreeing within a few tenths of a degree of the observed surface temperature. However, for surface temperature sensitivity studies, major differences between the two models can exist.

The differences result from the use of separate clear and cloudy sky water vapor profiles and from the coupling of cloud numbers, locations, and thicknesses to temperature. The interactive model's sensitivities to changes in the maximum altitude of convective extent, carbon dioxide, and surface relative humidity are presented. It is demonstrated that for global average conditions, the assumption of a constant distribution of relative humidity underestimates the water vapor amount and thermal contributions in radiative-convective models.

1. Introduction

As detailed in the review by Schneider and Dickinson (1974) climate modelling is an extremely difficult endeavor. Numerous, complex feedback mechanisms exist that are poorly understood and difficult to quantify for use in simple models. The intention of this research was to examine one of these mechanisms, the role of clouds in radiative-convective models.

Clouds are artificially located in the current generation of radiative-convective models. They are assigned specific pressure levels (Manabe and Wetherald, 1967), altitudes (Schneider, 1972; Cess, 1974; and Ramanathan, 1976), or the cloud top is held at a fixed temperature (Cess, 1974). The last two assumptions generally deal with radiative-convective models that utilize a single effective cloud and are known, respectively, as the constant cloud top height and constant cloud top temperature assumptions. The constant cloud top height is found by determining at what cloud height the radiative-convective model reproduces an assumed mean atmospheric temperature profile for an assumed set of input parameters. The height represents a height of best fit, not one based on physical considerations. The heights currently used are 5.5 km (Schneider, 1972), 6.8 km (Cess, 1974), and 6.25 km (Ramanathan, 1976). The constant cloud top temperature assumption was introduced by Cess (1974) as an alternative to fixing the cloud height; the cloud height changes in response to changes in the surface temperature. The temperature he suggested for a single effective cloud was 243.8 K, again chosen to reproduce a standard temperature profile. Reck (1979) recently

[1] Present affiliation: General Motors Research Laboratories, Physics Department, Warren, Michigan 48090, U.S.A.

0040-2826/81/040372-10$02.50/0

has demonstrated with a version of the Manabe and Wetherald model in use at the General Motors Research Laboratories that surface temperature sensitivities with the fixed cloud top temperature assumption are about 1.5 times higher than those with the fixed cloud top height assumption.

Manabe and Wetherald (1967) assign clouds to constant pressure levels, the levels and amounts based on the study by Telegadas and London (1954). The data are not a true representation of actual cloud distributions because the data are based entirely on oceanic observations. As noted by Telegadas and London (1954), this may lead to errors in the low cloud amounts which are influenced by local terrain. In addition, the data are not representative of diurnal averages. In their model, Manabe and Wetherald (1967) keep the cloud amounts fixed.

Weare and Snell (1974) developed a model that structures the atmosphere as a diffuse thin cloud. They allow the atmosphere to expand quasi-adiabatically and determine where saturation should occur. The cloud that is produced is assumed to be diffuse and to have a fractional cloudiness of one. Their cloud model includes rainout and produces water vapor mixing ratio profiles. In a later study, Temkin et al. (1975) used this model and two similar versions, one with an assumed 50% cloud coverage and one with a variable cloud coverage, to examine the effects on solar absorption in the earth–atmosphere system. They demonstrated that a model with variable cloud coverage has the largest surface temperature sensitivity to changes in solar absorption.

Present day large-scale computers do not as yet have the capacity to include a detailed radiation-dynamical model. In addition, the cloud patterns occur on a grid scale smaller than that of general circulation models so that some parameterization is required. As a result, studies involving surface temperature sensitivities to changes in CO_2, the solar constant (Manabe and Wetherald, 1975 and Wetherald and Manabe, 1975) or cloud amounts (Schneider et al., 1978) should be interpreted cautiously.

Roads (1978) has recently presented results on climate sensitivity to an atmospheric hydrologic cycle. His model includes transport of water vapor and condensed water and produces clouds whenever supersaturation occurs. His model predicts that cloud cover decreases about 1% for a 1 K increase in the surface temperature, in agreement with empirical results of Cess (1976).

Schneider et al. (1978), with the NCAR GCM, report that the effects on cloud cover amounts from surface temperature changes are latitudinally dependent. In their experiments for January conditions, the ocean surface temperature was changed globally and in zonal strips. The global ocean surface temperature changes led to low cloudiness changes of opposite sign. A zonal increase in ocean surface temperature in a strip centered at 15° N resulted in a cloudiness increase over the latitude strip and smaller decreases in adjacent latitude strips.

The model to be presented here interactively couples water vapor transport to a radiative-convective model. As the temperature profile changes in response to radiative heating or cooling, or latent heating, the distribution of water vapor is allowed to change in response to changes in the large-scale vertical velocity field and eddy diffusion. Clouds are formed whenever the atmosphere is saturated and the latent heat is released to the atmosphere. Although the total cloud cover is fixed at 50%, the number of cloud layers, their altitudes and thicknesses are computed. In addition, separate distributions of water vapor are computed for clear and cloudy conditions.

This model is used to examine the change in temperature brought about by changes in physical parameters such as carbon dioxide and surface relative humidity. The surface temperatures from this model are compared with those from a model with a fixed, single effective cloud with a water vapor profile based on a constant distribution of relative humidity in order to examine the impact of fixed cloud parameters and the neglect of the differences between water vapor distributions in clear and cloudy skies.

2. The radiation model

The radiation model used in this work is a compilation of those of Haurwitz and Kuhn (1974), Kuhn (1978), and Hummel and Kuhn (1981). The model includes the gases O_3, O_2, CO_2, and H_2O. The absorption properties were computed from a quasi-random band model (Wyatt et al., 1962) that utilizes a Voigt profile based on the work of Drayson (1976). The e-type water vapor absorption was included (Bignell, 1970). A total of 31 spectral intervals was used for the solar absorption by CO_2 and H_2O, 106 for O_2 and O_3 and photon fluxes were taken from Ackerman (1971). The spectral line data for the solar and infrared transmission functions were taken from McClatchey et al. (1973). The ozone densities were from Dopplick (1972) and a constant mass mixing ratio of 4.86×10^{-4} was assumed for CO_2. Overlapping by the spectral regions was included. The surface albedo was 14% (Hummel and Reck, 1979).

The model atmosphere was divided into the 12 levels listed in Table 1 at which the temperature was solved for by an initial value method that begins with an initial temperature profile and iterates to a steady-state solution. For details on the radiation model, the reader is referred to Hummel (1978). The model incorporates convective adjustment (Manabe and Strickler, 1964) to allow for the vertical redistribution of atmospheric internal energy, with pressure-dependent lapse rates based on critical moist adiabatic lapse rates (Stone and Carlson, 1979).

3. The water vapor transport model

The distribution of water vapor in the troposphere is to a large extent controlled by dynamics. In the radiative-convective models in use, water vapor is described by a constant distribution of relative humidity, $h(p)$ (Manabe and Wetherald, 1967), which differs from model to model but is typically of the form

$$h(p) = h_0 \left[\frac{p/p_0 - a}{1 - b} \right]^{\alpha} \tag{1}$$

where a, b, and α are constants and p is pressure. The surface value of relative humidity, h_0, is typically between 0.75–0.77. A water vapor distribution given by the above usually underestimates the amount of water vapor in the atmosphere. The annual average precipitable water described by the constant distribution of relative humidity is about 1.7 cm, 35% less than the value given by Starr et al. (1969) of 2.6 cm. As a result, the greenhouse effect is underestimated.

In an atmosphere with clouds, a distribution of relative humidity will not be very well approximated by (1). Throughout a cloud the relative humidity is 100%. Below the cloud the relative humidity generally decreases to the surface value. Therefore, we have used separate distributions of relative humidity to model average conditions, one for a clear sky and one for a cloudy sky. For clear sky conditions, a constant distribution of relative humidity given by (1) with $a = b = 0.02$ and $\alpha = 1$ is used. Whenever $h(p)$ is less than zero, the mixing ratio is set at 3×10^{-6} kg/kg. It will be shown that this distribution of $h(p)$ is in fact applicable for a clear sky atmosphere. For cloudy conditions, a water vapor transport model is used that includes large- and small-scale vertical velocities. When the computed water vapor density exceeds the saturation value, a cloud is assumed to be formed. A separate transport equation describes the liquid (solid) water content in the cloud region. The method predicts cloud height and thickness, the water vapor distribution above and below the cloud, and the distribution of condensed material within the cloud. Latent heat released is returned to the atmosphere. Multiple clouds (up to 3) can be handled in the radiation model. The model does not predict changes in cloud amount which is assumed to be 50%.

Transport of water vapor is given by

$$\frac{\partial^2 q}{\partial z^2} = \left[\frac{w}{K_z} + \frac{1}{H_\rho(z)} \right] \frac{\partial q}{\partial z} \tag{2}$$

where q is the water vapor mixing ratio; w, the large-scale vertical velocity; K_z, a mean eddy exchange coefficient; and $H_\rho(z)$ the density scale

Table 1. *Pressure levels used in the model calculations*

Level	Pressure (mb)
1	10
2	50
3	100
4	200
5	300
6	400
7	500
8	650
9	800
10	900
11	950
12	1000

height. The large-scale vertical velocity is assumed to be the velocity necessary to maintain hydrostatic equilibrium. The calculation is based on the Richardson equation (e.g. Dutton, 1976) in which all driving forces (i.e. pressure gradients, velocity divergences, heating terms, etc.) at a specific altitude are assumed to have a magnitude equal to the non-radiative heating rates necessary to maintain energy balance. The average vertical velocity produced under this assumption is on the order of 0.3–0.6 cm/s. The model calculations are very insensitive to the individual values of w and K_z and so average atmospheric values are used. Whenever the computed value of the mixing ratio exceeds the saturation value, the mixing ratio is assigned the saturation value. In this way, the region of the atmosphere where a cloud should exist can be specified. Equation (2) is solved numerically using a method equivalent to LU decomposition (Dahlquist et al., 1974). The mixing ratio at the surface, q_0, is given by the surface relative humidity h_0 and the surface temperature. The "top" of the model, or the extent over which water vapor is vertically transported is inputed. This assumed pressure level can be compared to the level of non-divergence in the atmosphere.

In the regions where clouds are predicted, the transport of liquid water is handled using a procedure employed by Hess (1976) to model the water vapor distribution on Mars. In his treatment, the large-scale velocity and scale height were neglected. If these terms are constant then Hess' transport equation has the form

$$\frac{\partial l}{\partial z} = \left(\frac{V}{K_z} + \frac{1}{H_\rho}\right) l + \left(\frac{w}{K_z} + \frac{1}{H_\rho}\right) q_s - \frac{\partial q_s}{\partial z} \tag{3}$$

where V is the terminal velocity of the droplets, assume constant, l is the mixing ratio of liquid (or solid) water, and q_s is the saturation water vapor mixing ratio. The above was solved by a 4th-order Runge-Kutta method. A value of 0.5 cm/s was used for the terminal velocity, which corresponds to an average radius of 6.5 μm. This value is representative of droplets found in typical clouds (Paltridge and Platt, 1976). The latent heat released following condensation or deposition is returned to the atmosphere and the temperature profile inside the clouds adjusted accordingly.

With the exception of the terminal velocity of the droplets, all of the relevant parameters were coupled to the temperature profile. The value of the water vapor mixing ratio at the surface was set equal to that for a relative humidity of 77%, in accordance with the constant relative humidity assumption used by Manabe and Wetherald (1967). While the model can generate multiple clouds, typically only one cloud was found in the equilibrium atmosphere.

The cloud and radiation models are coupled by first generating a set of clear sky heating/cooling rates which are used to determine w. The water vapor transport model gives the water vapor distribution and cloud heights. These are then used in the radiation program which computes a temperature profile in radiative-convective equilibrium with flux balance at the top of the atmosphere. The calculations are then repeated until the water vapor, clouds and temperature are self-consistent. The water vapor calculations are made at 37 equal height increments for the surface to the model top. These results are then interpolated onto the coarser grid used in the radiation program (see Table 1). Thus a thin cloud as calculated by the transport model may be represented as an infinitely thin cloud in the radiation program. The features of this model are compared to a number of other models in Table 2.

The equilibrium water vapor mixing ratio profile is shown in Fig. 1 for a 35° N, April atmosphere. The calculations were made with a model top of 450 mb and resulted in a thin cloud centered at 500 mb. Also shown is the profile resulting from the constant relative humidity assumption used for the clear sky distribution and the zonally averaged annual values reported by Starr et al. (1969). The average of the clear sky water vapor distribution and the cloudy sky result (with a model top at 450 mb) yielded the best agreement with the zonally averaged annual results of Starr et al. (1969). As will be demonstrated, the equilibrium temperature profile from the coupled radiation-transport model for this atmosphere gives the best agreement with standard atmosphere profiles. In addition, the equilibrium cloud is found at a height of 5.52 km in agreement with the constant cloud top height of 5.5 km employed by Schneider (1972).

For the sake of simplicity, the water vapor model results will be referred to as the cloudy sky profile and the constant relative humidity results, the clear sky profile. As shown in Fig. 1, the

Table 2. *Comparison of the cloud treatment in this model with other radiative-convective models*

	This work	Manabe and Wetherald (1967)	Ramanathan (1976)	Schneider (1972)	Weare and Snell (1974)
Number of cloud layers	Predicted (up to 3) and varies with $T(P)$	3 and constant	1 and constant	1 and constant	1
Cloud altitudes	Predicted and varies with $T(P)$	Fixed at constant pressure	Fixed at constant altitude	Fixed at constant altitude	Predicted
Cloud cover	Fixed	Fixed	Fixed	Fixed	Fixed
Water vapor profile	Separate clear and cloudy sky profiles—clear based on constant $h(P)$—cloudy based on vertical transport of water vapor	One profile based on constant $h(P)$	One profile based on constant $h(P)$	One profile based on constant $h(P)$	One profile

cloudy sky profile decreases with height. Hess (1976) and Paltridge and Platt (1976), in simpler cloud models, assumed that the water vapor mixing ratio below clouds was constant at the value at the surface. This assumption would lead to a lower cloud, the base occurring at about 2.0 km as opposed to 4.1 km as predicted by this model.

The clouds produced by this model are somewhat thicker and denser than observed clouds (Borovikov et al., 1963). The average liquid water content in the "standard" cloud shown in Fig. 1 was about 1.1×10^{-3} kg/m^3, in relative agreement with observed values (Borovikov et al., 1963; Fletcher, 1969). The shapes of the liquid water profiles are similar to observed profiles, increasing to a maximum near the cloud center.

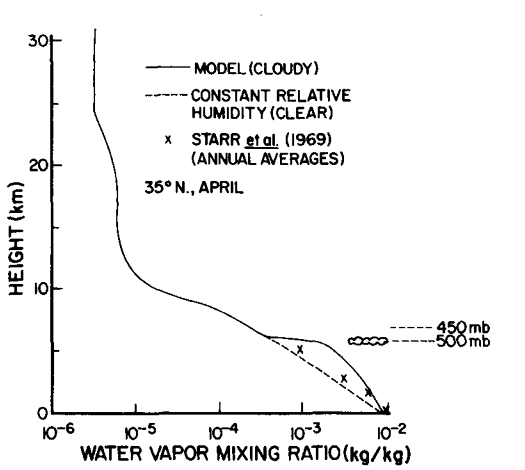

Fig. 1. Water vapor profiles from the water vapor transport model and the assumption of a constant distribution of relative humidity.

Finally, the total atmospheric water vapor profile, which is the average of the clear and cloudy results, agrees well with the results of Starr et al. (1969). The precipitable water amount for the atmosphere is 2.7 cm, about 4% higher than the annual results of 2.6 cm reported by Starr et al. (1969). While Weare and Snell (1974) did not give a value for the precipitable water, their value would be higher than ours because of their nearly constant water vapor mixing ratio below the cloud and because they did not include a separate, clear sky profile.

4. Results

The water vapor and radiation models were coupled by first assuming an initial temperature profile and then calculating the water vapor distribution. As described in the previous section, separate water vapor distributions were used for the clear and cloudy sky cases. The transmission functions were then computed for all of the gaseous constituents. Separate flux calculations were performed for the clear and cloudy atmospheres and weighted by the respective clear and cloud covered fractional amounts (50%). In those regions of the atmosphere where convective adjustment was not required, radiative equilibrium was required for convergence. If equilibrium did not exist, an iteration was made on the flux calculations until radiative equilibrium was achieved. A balance between the incoming solar and outgoing infrared radiation, which is applicable for 35° N, April and global conditions (Vonder Haar and Suomi, 1971), was checked for. If there was agreement to within ±0.5%, the calculations were terminated. Otherwise, the surface temperature was adjusted, a new temperature profile computed, and new water vapor profiles generated for both the clear and cloudy atmospheres. New transmission functions were computed and the flux calculations repeated until the radiative equilibrium and flux balance criteria were met.

The upper boundary of the water vapor model which can be related to the top of the region of convective activity was varied in order to determine its influence on cloud height and surface temperature. A series of tests was made with the model top set at 200, 300, 450, and 650 mb and the results are summarized in Table 3. As shown, the higher the model top the greater the vertical extent of the clouds. For clouds with tops at 200 and 300 mb the resulting cloud extents and liquid water contents are representative of intense cumuliform clouds. It is noted, though, that this model makes no attempt to predict specific types of clouds or their coverage. As the cloud top heights increased, the surface temperatures increased as predicted by Schneider (1972), among others. The higher surface temperature results from two factors. First, the higher the cloud top height, the lower the temperature at which the cloud top radiates to space. Second, as the surface temperature increases, the amount of atmospheric vapor increases, thereby increasing the amount of water vapor absorption. The net effect is that the outgoing infrared flux is decreased, forcing the surface temperature to increase. The clouds vanished when the model top was put at 650 mb.

Table 3. *Surface temperatures and cloud extents for various water vapor model tops*

Top of water vapor model (mb)	Surface temperature (K)	Extent of cloud (mb)
200	304.7	500–200
300	299.8	500–300
450	289.6	500–500
650	292.5	Clear sky

The resulting water vapor distribution from the 650 mb model top agreed quite closely with the profile (1) produced from the assumption of a constant relative humidity distribution.

The surface temperature resulting from a model top of 200 mb is unrealistic. The equilibrium atmosphere for this case contains about 9 cm of precipitable water, about a factor of 3 larger than that expected for annual global conditions (Sellers, 1965; Starr et al., 1969). This result points out a deficiency in the water vapor transport model. The model assumes no coupling between surface temperature and relative humidity. In the cloudy atmosphere, the relative humidity distribution is computed, but in the clear atmosphere the distribution is held fixed. In addition, the surface value of relative humidity in the clear and cloudy atmospheres is the same.

As shown in Table 3, a model top at 450 mb gives the most realistic surface temperature. The complete profile is shown in Fig. 2. The cloud top occurs about 5.5 km. This height agrees with the effective cloud top height used by Rasool and Schneider (1971) and Schneider (1972) and is close to the effective cloud top heights of 6.25 and 6.8 km used by Ramanathan (1976) and Cess (1974), respectively. The model atmosphere with a 450 mb model top will be used as the "standard" atmosphere for the following comparisons.

The sensitivity of the model to the surface relative humidity is summarized in Table 4. Lowering the surface relative humidity reduces the

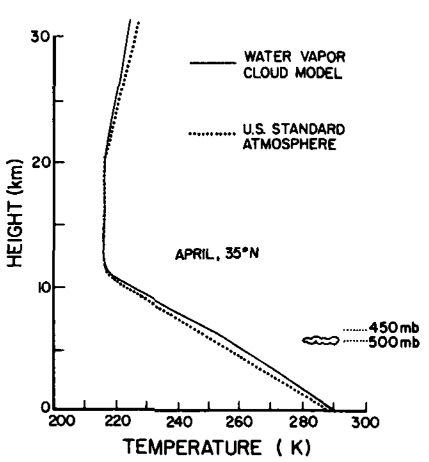

Fig. 2. Comparison of equilibrium profiles from the interactive water vapor model, and the U.S. Standard Atmosphere.

Table 4. *Summary of the model atmosphere's response to changes in surface relative humidity*

	Water vapor transport		
		Cloud extent (mb)	
Surface relative humidity (%)	Surface temperature (K)	Top	Base
50	288.73	Clear sky	
67	289.39	500	500
77	289.61	500	500
90	291.06	500	650

water vapor content and leads to a decrease in the infrared cooling and solar heating by water vapor. The net outgoing infrared flux increases and the surface temperature decreases to maintain flux balance. With the standard conditions of 77% relative humidity the steady-state cloud is about 1.7 km thick centered at 500 mb. For a surface relative humidity of 67% the cloud is only 0.8 km thick and at 55% relative humidity the cloud is about 0.5 km thick. A relative humidity of 50% produces a cloud-free atmosphere. Conversely, a larger surface relative humidity causes the cloud to be thicker.

The significance of separate water vapor profiles for the calculation of clear and cloudy conditions is demonstrated in Table 5. For the cloudy atmosphere, the mixing ratio at the surface is set equal to that in the clear sky, but the distribution of water vapor in height is calculated from the transport model. For clear sky calculations the relative humidity is given by (1). Weighting the fluxes from the two calculations by the cloud cover (50%) then yields the temperatures designated Fully Interactive. The column labeled Floating Clouds Only (FCO) refers to the radiative-convective model with cloud altitudes and thicknesses predicted using the transport equation (2) but with the same distribution of relative humidity (1) for both the clear and cloudy calculations.

The FCO results yield a lower surface temperature than the fully interactive model and two thin clouds occur rather than one. The importance of the dual water vapor profiles is demonstrated even more clearly for a 90% surface relative humidity. The cloud is thicker in the FCO model and the sensitivity to surface temperature is 4.0 K, about 3.3 times larger than that from the fully interactive model. The FCO results with doubled CO_2 also yield a lower surface temperature but have a larger sensitivity to doubled CO_2 being 1.2 K as opposed to 0.8 K for the fully interactive model.

5. Discussion

The present model has similarities to that of Weare and Snell in that both predict cloud height. However, Weare and Snell do not explicitly include the vertical transport of water vapor as we have done, but rather define an "entropy parameter" such that the atmospheric lapse rate is 6.5 K/km whenever the temperature is above the dew point; in our model the radiation field determines the temperature when saturation does not occur, otherwise the moist adiabatic lapse rate is used. Also in their model the cloud cover

Table 5. *Comparison of surface temperatures and cloud properties predicted with a model (fully interactive) including both clear and cloudy sky water vapor profiles and a model (floating clouds only) that predicts cloud locations but uses a single water vapor profile based on a constant distribution of relative humidity*

	Fully interactive		Floating clouds only	
Conditions	Surface temperature (K)	Cloud extent (mb)	Surface temperature (K)	Cloud extent (mb)
77% RH, 1 (CO_2)	289.9	500–500	289.0	500–500 650–650
77% RH, 2 (CO_2)	290.7	500–500	290.2	500–500 650–650
90% RH, 1 (CO_2)	291.1	500–650	293.0	400–650

is 100% but the cloud is diffuse while in ours the cloud is opaque, the coverage is 50% and there are separate calculations for the clear and cloudy sky, the radiation fluxes then being weighted by the cloud cover to yield the final temperature. There is no detailed treatment in the Weare and Snell model of the radiative transfer, particularly with regard to solar absorption, and our treatment of the radiation is more similar to that of Manabe and Wetherald. However, we have included absorption by the water vapor dimer, the explicit temperature dependence of the absorption bands, and a finer spectral resolution. The numerical technique to determine radiative convective equilibrium is the same as Manabe and Wetherald's (1967). Also we use a critical moist adiabatic lapse rate while Manabe and Wetherald use 6.5 K/km and their cloud heights and thicknesses are specified.

The surface temperature, water vapor profiles, and precipitable water representative of observed conditions are predicted by the model when the water vapor transport model top is 450 mb. The calculated surface temperature is 289.6 K and the corresponding precipitable water amount 2.7 cm. This compares well with the annual results of 2.6 cm and 2.5 cm reported by Starr et al. (1969) and Sellers (1965) respectively. Previous studies generally used a constant distribution of relative humidity given by (1) and we find that this distribution gives considerably less water vapor than predicted from our model. Below the cloud base the clear sky mixing ratio can be as much as a factor of two less than the cloudy sky value. As a result the amount of precipitable water is underestimated. For standard atmospheric conditions, the precipitable water is calculated to be only 1.7 cm when a constant relative humidity is used for the cloudy sky as well as clear sky case. Thus the greenhouse effect will be underestimated. Weare and Snell do not give the precipitable water in their model although it would be somewhat larger than we find; the mixing ratios are the same at the surface but our values decrease more rapidly with height. Their condensed water density is about two orders of magnitude less than that in actual clouds.

The temperature increase for a doubling of CO_2 from this model is 0.8 K. As summarized by Schneider (1975) the range of predicted increase from various models is 0.7 to 3.0 K, the lower value reported by Weare and Snell (1974). Although our predicted increase is close to their value, and both studies included cloud cover, the agreement is probably fortuitous since the specified critical lapse rates and cloud covers are different. Recently Manabe and Wetherald (private communication) calculated a temperature increase of 1.9 K; however, their model contains three cloud layers with fixed height and thickness and a critical lapse rate of 6.5 K/km.

There is still much improvement to be made in 1D models and although we have succeeded in coupling a "cloud generation" model with a detailed radiation code, the cloud cover has been specified. Also the model assumes no coupling between surface temperature and relative humidity. The three-dimensional results of Wetherald and Manabe (1975) and Roads (1978) suggest this is highly nonlinear.

6. Acknowledgements

This work was supported by NASA under Grant NSF 7209 from the Upper Atmosphere Research Program and the Department of Energy (Carbon Dioxide and Climate Research Program).

REFERENCES

Ackerman, M. 1971. Ultraviolet solar radiation related to mesospheric processes. In *Mesospheric models and related experiments* (ed. G. Fiocco), 149.

Bignell, K. J. 1970. The water-vapour infra-red continuum. *Quart. J. Roy. Met. Soc. 96*, 390–403.

Borovikov, A. M., Gaivornoskii, I. I., Zak, E. G., Kostariv, V. V., Mazin, I. P., Minervin, V. E., Khrgian, A. Kh. and Shmeter, S. M. 1963. *Cloud physics*. Israel Program for Scientific Translations, Jerusalem, 392 pp.

Cess, R. D. 1974. Radiative transfer due to atmospheric water vapor: Global considerations of the earth's energy balance. *J. Quant. Spectrosc. Radiat. Transfer 14*, 861–871.

Cess, R. D. 1976. Climate change: An appraisal of atmospheric feedback mechanisms employing zonal climatology. *J. Atmos. Sci. 33*, 1831–1843.

Dahlquist, G., Bjork, A. and Anderson, N. 1974. *Numerical methods*. New York: Prentice-Hall, 573 pp.

Dopplick, T. G. 1972. Radiative heating of the global atmosphere. *J. Atmos. Sci. 29*, 1278–1294.

Drayson, S. R. 1976. Rapid computation of the Voigt profile. *J. Quant. Spectrosc. Radiat. Transfer 16*, 611–614.

Dutton, J. A. 1976. *The ceaseless wind.* New York: McGraw-Hill, 579 pp.

Fletcher, N. H. 1969. *The physics of rainclouds*, Cambridge: University Press, 390 pp.

Haurwitz, F. and Kuhn, W. R. 1974. The distribution of tropospheric planetary radiation in the southern hemisphere. *J. Applied Meteor. 13*, 417–429.

Hess, S. L. 1976. The vertical distribution of water vapor in the atmosphere of Mars. *Icarus 28*, 269–278.

Hummel, J. R. 1978. An atmospheric radiative-convective model with interactive water vapor transport and cloud development. Ph.D. Dissertation, Univ. of Michigan.

Hummel, J. R. and Kuhn, W. R. 1981. Comparison of radiative-convective models with constant and pressure dependent lapse rates. Submitted to *Tellus 33*.

Hummel, J. R. and Reck, R. A. 1979. A global surface albedo model. *J. Appl. Meteor. 18*, 239–253.

Kuhn, W. R. 1978. The effects of cloud height, thickness, and overlaps on tropospheric terrestrial radiation. *J. Geophys. Res. 83*, 1337–1346.

McClatchey, R. A., Benedict, W. S., Clough, S. A., Burch, D. E., Calfee, R. F., Fox, K., Rothman, L. S. and Garing, J. A. 1973. AFCRL atmospheric absorption line parameters compilation. *Environ. Res. Pa. 34*. Hanscom Air Force Base, Bedford, Massachusetts: Air Force Cambridge Res. Lab.

Manabe, S. and Strickler, R. F. 1964. Thermal equilibrium of the atmosphere with a convective adjustment. *J. Atmos. Sci. 21*, 361–385.

Manabe, S. and Wetherald, R. T. 1967. Thermal equilibrium of the atmosphere with a given distribution of relative humidity. *J. Atmos. Sci. 24*, 241–259.

Manabe, S. and Wetherald, R. T. 1975. The effects of doubling the CO_2 concentration on the climate of a general circulation model. *J. Atmos. Sci. 32*, 3–15.

Paltridge, G. W. and Platt, C. M. R. 1976. *Radiative processes in meteorology and climatology*. New York: Elsevier Scientific Pub. Co., 318 pp.

Ramanathan, V. 1976. Radiative transfer within the earth's troposphere and stratosphere: A simplified radiative-convective model. *J. Atmos. Sci. 33*, 1330–1346.

Rasool, S. I. and Schneider, S. H. 1971. Atmospheric carbon dioxide and aerosols: Effects of large increases in global climate. *Science 173*, 138–141.

Reck, R. A. 1979. Comparison of fixed cloud-top temperature and fixed cloud-top altitude approximations in the Manabe–Wetherald radiative-convective atmospheric model. *Tellus 31*, 400–405.

Roads, J. A. 1978. Numerical experiments on the climatic sensitivity of an atmospheric hydrologic cycle. *J. Atmos. Sci. 35*, 753–773.

Schneider, S. H. 1972. Cloudiness as a global climatic feedback mechanism: The effects on the radiation balance and surface temperature of variations in cloudiness. *J. Atmos. Sci. 29*, 1413–1422.

Schneider, S. H. and Dickinson, R. E. 1974. Climate modeling. *Rev. Geophys. Space Phys. 12*, 447–493.

Schneider, S. 1975. On the carbon dioxide-climate confusion. *J. Atmos. Sci. 32*, 2060–2066.

Schneider, S. H., Washington, W. M. and Chervin, R. M. 1978. Cloudiness as a climatic feedback mechanism: Effects on cloud amounts of prescribed global and regional surface temperature changes in the NCAR GCM. *J. Atmos. Sci. 35*, 2207–2221.

Sellers, W. C. 1965. *Physical climatology*. Chicago: The University of Chicago Press, 272 pp.

Starr, V. P., Peixoto, J. P. and McKean, R. G. 1969. Pole-to-pole moisture conditions for the IGY. *Pure Appl. Geophys. 73*, 85–116.

Stone, P. H. and Carlson, J. H. 1979. Atmospheric lapse rate regimes and their parameterization. *J. Atmos. Sci.* 415–423.

Telegadas, K. and London, J. 1954. A physical model of the northern hemisphere troposphere for winter and summer. Dept. of Meteorology, New York University, AF 19(122) 165.

Temkin, R. L., Weare, B. C., and Snell, F. M. 1975. Feedback coupling of absorbed solar radiation by three model atmospheres with clouds. *J. Atmos. Sci. 32*, 873–880.

Vonder Haar, T. H. and Suomi, V. E. 1971. Measurements of the earth's radiation budget from satellites during a five-year period. Part I: Extended time and space means. *J. Atmos. Sci. 28*, 305–314.

Weare, B. C. and Snell, F. M. 1974. A diffuse thin cloud structure as a feedback mechanism in global climatic modeling. *J. Atmos. Sci. 31*, 1725–1734.

Wetherald, R. T. and Manabe, S. 1975. The effects of changing the solar constant on the climate of a general circulation model. *J. Atmos. Sci. 32*, 2044–2059.

Wyatt, P. J., Stull, V. R. and Plass, G. N. 1962. Quasi-random model of band absorption. *J. Opt. Soc. Am. 52*, 1209–1217.

АТМОСФЕРНАЯ РАДИАЦИОННО-КОНВЕКТИВНАЯ МОДЕЛЬ СО ВЗАИМОДЕЙСТВУЮЩИМИ ПЕРЕНОСОМ ВОДЯНОГО ПАРА И РАЗВИТИЕМ ОБЛАКОВ

В современном поколении радиационно-конвективных моделей облакам приписываются определенные уровни или температуры, которые не изменяются в ходе расчетов. Кроме того, используется единое распределение водяного пара для "средней атмосферы" вместо отдельных распределений дли безоблачной и облачной атмосфер. Авторы представляют результаты одномерной радиационно-конвективной модели, которая включает взаимодействующий перенос водяного пара и предсказывает высоты и толщины облаков.

Полностью взаимодействующая модель и модель с одним фиксированным облаком и одним профилем водяного пара обе могут воспроизводить среднеглобальный профиль температуры, их поверхностные температуры согласуются в пределах нескольких десятых градуса с наблюдаемой поверхностной температурой. Однако, для исследований чувствительности поверхностной температуры могут существовать большие различия между двумя моделями.

Различия являются результатом использования отдельных профилей водяного пара для облачного и безоблачного неба и результатом связи количества облаков, их положении и толщин с температурой. В работе представлены чувствительности моделей со взаимодействием на изменения верхней границы конвективного слоя, изменения двуокиси углерода и поверхностной относительной влажности. Показано, что для среднеглобальных условий предположение постоянного распределения относительной влажности недооценивает вклады количества водяного пара и тепла в радиационно-конвективные модели.